Nanoscale

Accepted Manuscript

This article can be cited before page numbers have been issued, to do this please use: D. Chen, R. qiao, X. Xu, W. Dong, L. Wang, R. Ma, C. Liu, Z. Zhang, M. Wu, L. Liu, L. Bao, H. Wang, P. Gao, K. Liu and D. Yu, *Nanoscale*, 2019, DOI: 10.1039/C9NR00412B.

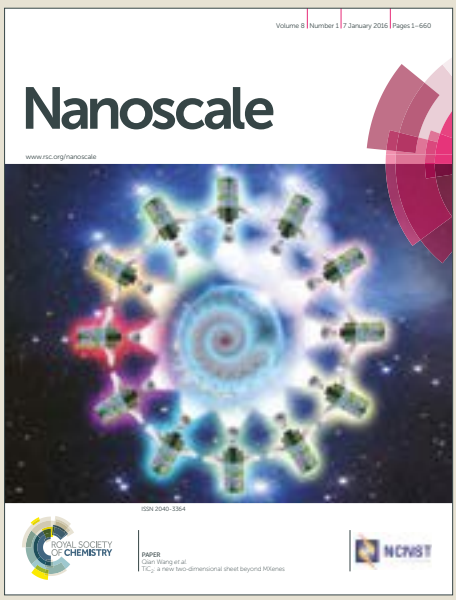

ROYAL SOCIETY OF CHEMISTRY

rsc.li/nanoscale

View Article Online
DOI: 10.1039/C9NR00412B

Nanoscale

COMMUNICATION

Sub-10 nm Stable Graphene Quantum Dots Embedded in Hexagonal Boron Nitride†

Received 00th January 20xx,
Accepted 00th January 20xx

DOI: 10.1039/x0xx00000x

www.rsc.org/

Dongxue Chen,‡[abc] Ruixi Qiao,‡[b] Xiaozhi Xu,[b] Weikang Dong,[d] Li Wang,[be] Ruisong Ma,[e] Can Liu,[b] Zhihong Zhang,[b] Muhong Wu,[b] Lei Liu,[f] Lihong Bao,[e] Hui-Tian Wang,[c] Peng Gao,[d] Kaihui Liu*[b] and Dapeng Yu*[ag]

Graphene quantum dots (GQDs), a zero-dimensional material system with distinct physical properties, have great potentials in the applications of photonics, electronics, photovoltaics, and quantum information. Especially, GQD is one of promising candidates for quantum computing. In principle, sub-10 nm size is required for GQDs to present the intrinsic quantum properties. However, with such extreme size, GQDs have predominant edges with lots of active dangling bonds and thus are not stable. Satisfying the demands of both quantum size and stability is therefore of great challenge in the design of GQDs. Herein we demonstrate the fabrication of sub-10 nm stable GQD array by embedding them into large-bandgap hexagonal boron nitride (h-BN). With this method, the dangling bonds of GQDs were passivated by surrounding h-BN lattice to ensure high stability, meanwhile maintaining their intrinsic quantum properties. The sub-10 nm nanopore array was first milled in h-BN by advanced high-resolution helium ion microscope and then GQDs were directly grown in them through chemical vapour deposition process. Stability analysis proved that the imbedded GQDs show negligible property decay after baking at 100 ℃ in air for 100 days. The success in preparing sub-10 nm stable GQD array will promote the physical exploration and potential applications in this unique zero-dimensional in-plane quantum material.

Introduction

Among broad low-dimensional materials,[1-3] zero-dimensional quantum dots are an important family member that present rich quantum properties and wide applications.[4, 5] As an emerging in-plane zero-dimensional material originated from the star material of two-dimensional graphene, graphene quantum dots (GQDs) exhibit rich superior properties to conventional semiconductor quantum dots.[6-22] Theoretical calculations reveal that a large tunable bandgap from 0 eV of infinite graphene sheets to ~7 eV of benzene can be accurately engineered for GQDs by varying their size and morphology.[7, 8] Weak spin-orbit coupling and absence of hyperfine interaction of carbon-based materials provide GQDs possibilities for spin qubits with long coherence times up to 100 ns.[9] GQDs were also reported to show low cytotoxicity, excellent biocompatibility and environmental friendliness in contrast with conventional semiconductor quantum dots made from toxic heavy metals.[10] All of these intriguing properties make GQDs a promising material for optoelectronics,[11] photonics,[12, 13] biomedicine,[14, 15] electronics,[16-20] and quantum computation.[21, 22] In principle, to exhibit the intrinsic quantum properties of GQDs, their size must shrink into the range of typically sub-10 nm to ensure the strong quantum confinement.[6, 10] However, once the size reaches sub-10 nm scale, the predominant edges with lots of active dangling bonds make GQDs unstable.[23-26] It seems that quantum size and stability of GQDs are incompatible with each other.

In the past 10 years, great efforts have been tried to fabricate sub-10 nm-scale stable GQDs. One prevailing strategy is to decompose or exfoliate the bulk graphite into graphene flakes by chemical or physical routes like hydrothermal cutting, electrochemical cutting, microwave-assisted or ultrasonic shearing.[27-31] However, in these methods, the GQDs have large size distribution and lots of chemical species reconstructed and adsorbed on the dangling bonds of the GQDs edges, which prevent the presence of their intrinsic quantum properties. Another strategy is based on the high-resolution lithography on graphene film. With this technique, one can precisely cut

[a] Institute for Quantum Science and Engineering and Department of Physics, Southern University of Science and Technology, Shenzhen 518055, China.
[b] State Key Laboratory for Mesoscopic Physics, Collaborative Innovation Center of Quantum Matter, School of Physics, Peking University, Beijing 100871, China.
[c] School of Physics, Nankai University, Tianjin 300071, China.
[d] Electron Microscopy Laboratory, School of Physics, Peking University, Beijing 100871, China
[e] Institute of Physics, Chinese Academy of Sciences, Beijing 100190, China
[f] Department of Materials Science and Engineering, College of Engineering, Peking University, Beijing 100871, China
[g] Shenzhen Key Laboratory of Quantum Science and Engineering, Shenzhen 518055, China

† Electronic Supplementary Information (ESI) available: Measurement of EELS, STEM characterization. See DOI: 10.1039/x0xx00000x

‡ These authors contributed equally to this research work.

graphene to designed size and shape, thus producing uniform GQDs.[32] But the size obtained is typically above tens of nanometres (due to the resolution limit in conventional lithography fabrication), and the GQDs edges are unstable. Chemical vapour deposition (CVD) method was also applied to grow GQDs directly, but the obtained size is still in the order of 100 nm to microns.[33] Therefore, how to fabricate GQDs with both quantum size and high stability is still of great challenge till now.

Here for the first time, we demonstrate the fabrication of sub-10 nm GQD array with high stability of more than 100 days at 100 ℃. The starting point of our design is to embed GQDs into a lattice-matching material to passivate the dangling bonds of GQDs to ensure stabilization. Meanwhile, this material should be a large-bandgap insulator to maintain intrinsic properties of GQDs. Hexagonal boron nitride (h-BN), a high-profile 2D insulating material with a wide bandgap of ~6 eV, is chosen for this purpose as it has the same lattice symmetry and similar lattice constant with graphene (only 1.7% mismatch).[33-36] We utilized the high-resolution fabrication ability of helium ion microscope (HIM) to directly mill sub-10 nm nanopore array on h-BN and followed by CVD method to grow GQDs inside these nanopores. The successful fabrication of sub-10 nm stable GQD array will promote their practical applications and physical exploration in this zero-dimensional in-plane quantum material.

Results and discussion

In our experiment, h-BN flakes were first capped onto a Cu foil by mechanical exfoliation method. Then the nanopore array was directly milled on these flakes by an advanced focused helium ion microscope with sub-nanometre resolution (Fig. 1a). Compare with the traditional gallium ion beam microscope, in helium ion microscope helium has much smaller mass and therefore gives much better spatial resolution.[37, 38] Afterwards, the GQDs were synthesized into these nanopores to form the GQDs-BN embedded structure (Fig. 1b) by low pressure chemical vapour deposition (see Experimental Section for more details of the growth process). Finally, the synthesized GQDs were transferred onto SiO2/Si or other target substrates for further characterization (Fig. 1c). With this technique, one can accurately fabricate nanopore array with designed size (as small as 4 nm) and patterns (Fig. 1d-f).

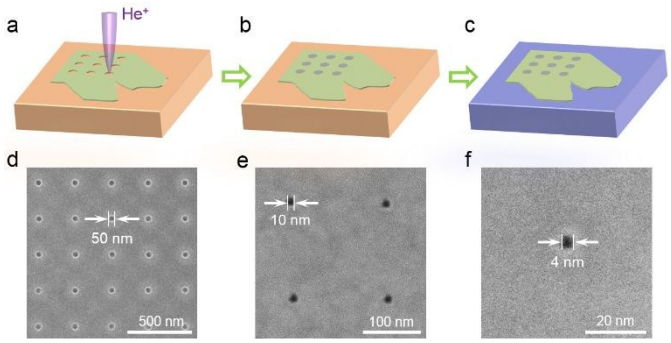

Fig. 1 Schematic diagrams of (a) helium ion microscope-based fabrication of nanopore array on h-BN, (b) synthesis of GQD array embedded in h-BN, (c) GQD array embedded in h-BN transferred to other substrate. (d-f) Nanopores on h-BN with diameters of 50 nm, 10 nm and 4 nm, respectively.

To check the quality of as-grown GQDs, Raman spectroscopy was first conducted after the material was transferred onto SiO2/Si substrate. For the area without h-BN flakes, the characteristic G mode and 2D mode of graphene can be observed (olive curve shown in Fig. 2a). The 2D/G intensity ratio of ~2 and the weak D mode demonstrate that high-quality monolayer graphene is synthesized on the Cu surface without h-BN flakes. Raman spectrum on bare h-BN only shows E2g mode of h-BN at 1374 cm-1 without any detectable signal of graphene (orange curve shown in Fig. 2a), revealing the absence of epitaxial graphene growth above or below of h-BN under our growth conditions. In contrast, as to Raman spectrum on GQDs region (dark yellow curve shown in Fig. 2a), the E2g mode of h-BN as well as the G and 2D mode of graphene co-exist, revealing that graphene is indeed grown in the nanopores of h-BN (laser spot size is larger than GQDs size). The appearance of D and D' mode should be attributed to edges of GQDs.[39, 40]

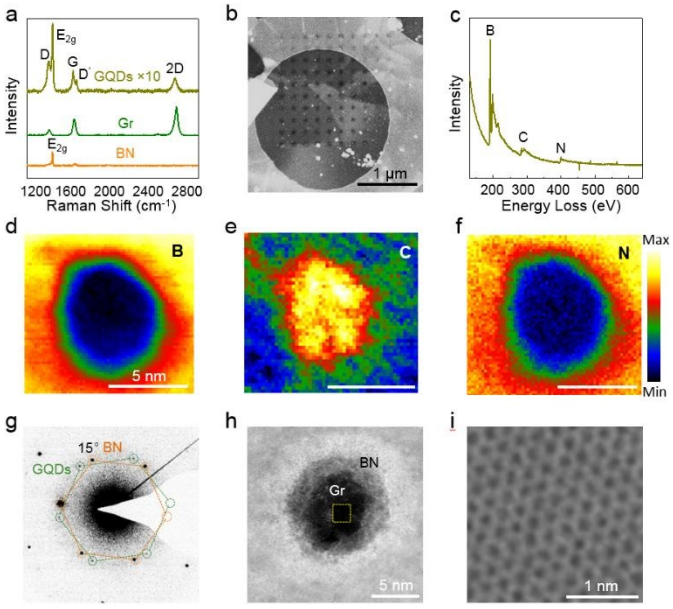

Fig. 2 (a) Raman spectra of h-BN (orange), graphene (olive) and GQD array embedded in h-BN flake (dark yellow), respectively. (b) Low magnification STEM image of GQD array in h-BN nanopores. The circle in this Fig. is hollow carbon film of TEM grids. (c) EELS spectrum of GQD array embedded in h-BN. (d-f) Corresponding EELS mapping of boron, carbon and nitrogen in (c) under STEM mode. (g) SAED pattern of a GQD embedded in h-BN. (e) STEM image of GQDs and h-BN heterojunction. (h) An atomically-resolved image of the GQDs in the area marked by yellow box in (i).

To further confirm the embedded GQDs-BN structure, the as-grown sample was transferred onto holey carbon film transmission electron microscope (TEM) grids (Fig. 2b) and characterized by electron energy loss spectroscopy (EELS). The detected peaks (Fig. 2c; ESI Fig. S1 †) verify the chemical components of boron, carbon and nitrogen.[41-43] Further EELS mapping of boron (Fig. 2d), carbon (Fig. 2e) and nitrogen (Fig. 2f) under STEM mode provide an unambiguous evidence for the existence of GQDs inside h-BN. Then we carried out selected-

area electron diffraction (SAED) and scanning transmission electron microscopy (STEM) to investigate the structural information of the GQD array in both the reciprocal space and real space. The diffraction pattern shows two sets of hexagonal diffraction patterns with ~15° twist angle (Fig. 2g), corresponding to graphene and h-BN lattices (electron beam area is larger than GQDs size).[34] The STEM images of graphene show atomically-resolved carbon hexagons (Fig. 2g-i; ESI Fig. S2†), demonstrating that GQDs have been successfully embedded in the nanopores of h-BN.

By milling nanopores on exfoliated h-BN, we successfully realized the fabrication of GQDs in sub-10 nm. However, these exfoliated h-BN flakes are of small size and cannot meet the demand of large-scale applications. Thus, to push this method to large-size h-BN films is very significant for further real applications. To verify the universality of our method, CVD grown h-BN monolayer was used[44] and nanopores with typical size of ~4 nm were milled by the same procedure as that on exfoliated h-BN flakes (Fig. 3a-b). Raman spectroscopy showed that GQDs were also synthesized in the nanopores of CVD-grown h-BN monolayer (Fig. 3c). The GQD array was transferred onto holey carbon film TEM grids supported by monolayer graphene film and characterized by TEM (CVD-grown h-BN monolayer is fragile if without the support of graphene film). The SEAD pattern shows the signal of both GQDs and graphene film in Fig. 3d-e (electron beam area is smaller than GQDs size here). The high-resolution transmission electron microscopy (HRTEM) image shows Moiré lattice of GQDs on the graphene film (Fig. 3f) and the Moiré period of ~1.17 nm is consistent with the twist angle of ~12° as in the SEAD. These characterizations demonstrate unambiguously that GQDs were embedded into the nanopores of CVD-grown h-BN monolayer.

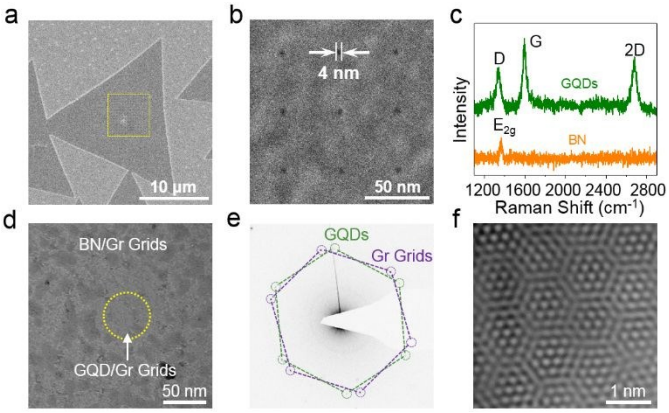

Fig. 3 (a) Helium ion microscopic image of nanopore array milled on CVD-grow h-BN monolayer. (b) Helium ion microscopic image of nanopore array with diameter of 4 nm. (c) Raman spectra of h-BN (orange) and GQD array embedded in h-BN (olive). (d) A low-magnification TEM image of GQDs (yellow dotted circle) embedded in CVD-grown h-BN as supported by a graphene TEM film. (e) SAED pattern of GQDs shown in (d). (f) HRTEM image of Moiré pattern of GQDs and graphene TEM film shown in (d).

As the edges and dangling bonds were passivated by surrounding h-BN lattices, the stability of as-grown GQDs should be greatly improved. To verify this expectation, a comparative experiment of stability between commercially available GQDs (~5 nm in diameter) and our embedded GQDs was conducted. For the commercial GQDs, the signal from Raman spectrum is too weak to detect the stability even after heating in air at 100 ℃ for only 5 mins (Fig. 4a). However, it is much easier to distinguish the variation by high intensity signal from photoluminescence (PL). The intensity of the PL peak declined sharply within a few minutes after heating in air at 100 ℃ (Fig. 4b). In just 5 minutes, the intensity dropped to one-tenth of its original level and became undetectable in 60 minutes. At lower temperature of 90 ℃ or 80 ℃, continuously tracked PL intensity shows obvious decrease as well (Fig. 4c), suggesting the instability of conventional isolated GQDs. Here we note that the intrinsic bandgap of GQDs with diameter of 5 nm should be around 0.2 eV (6200 nm in PL spectrum) from equation ΔE (eV) ≈ 1/D (nm),[45, 46] where D is the diameter of the GQD, and the observed PL in commercial GQDs in the visible range is a signature for the presence of extrinsic quantum effects likely due to the unsaturated edges adsorbed with nitrides and sulphides (ESI Fig. S3†). This observation is consistent with previous reports that the ordinary GQDs will have extrinsic quantum effects due to the adsorption of chemical species or functional group.[47-49] Instead, our GQDs show clear Raman feature of graphitic materials but no PL in the visible range (Fig. 4d). While for our GQDs embedded in h-BN, the Raman spectra keep almost invariable even after heating in air at 100 ℃ for 100 days (Fig. 4e-f), revealing the great stability of our GQD materials.

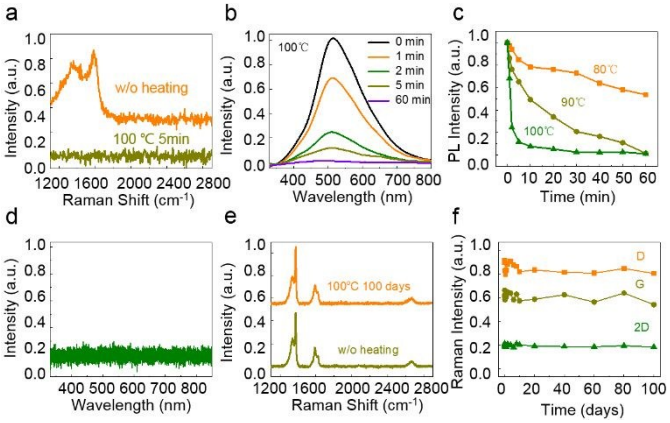

Fig. 4 (a) Raman spectrum of commercial GQDs. (b) Photoluminescence spectra of commercial GQDs baked in air with different time at 100 ℃. (c) The intensity evolution of photoluminescence spectra of commercial GQDs baked at different temperatures. (d) Photoluminescence spectrum of GQDs embedded in h-BN. (e) Raman spectra of GQDs embedded in h-BN baked at 100 ℃ before (dark yellow) and after 100 days (orange). (f) The intensity evolution of D, G and 2D mode of GQDs during baking in air at 100 ℃ with different time.

Conclusions

The success in preparing the sub-10 nm stable GQD array in both exfoliated h-BN flakes and CVD-grown h-BN monolayer will promote the large-scale applications of GQDs. For example, with lower atomic weight of GQDs, the coherence times of spin qubits could increase due to weak spin-orbit coupling and the absence

of hyperfine interaction of carbon, which makes GQDs a promising candidate for quantum computation. In addition, the embedding technique combined with high-resolution fabrication of helium ion microscope may pave new directions for other air-stable quantum materials from broad two-dimensional materials, such as transitional metal dichalcogenides, silicene, stanene, germanene, phosphorene and so on, and therefore establish a broad materials system of zero-dimensional in-plane quantum dots with sub 10 nm size and good stability.

Experimental

GQDs growth

GQDs was grown in a tube furnace (Hefei Kejing Co. Ltd.) by CVD at pressure about 200 Pa. The CVD system was gradually heated up to 1000 ℃ for exfoliated h-BN or 850~1000 ℃ for CVD-synthesized h-BN under 50 sccm Ar and 2 sccm H2. 10 sccm of CH4 was introduced during the growth of GQDs for 5 min. After growth, the CVD system was cooled down to room temperature quickly under the protection of mixed Ar and H2 flow.

h-BN preparation

The mechanically exfoliated h-BN was directly capped onto a copper (25μm thick, 99.8%, Sichuan Oriental Stars Trading Co. Ltd.). The CVD-synthesized h-BN was grown on the same type of copper with ammonia borane (NH3–BH3) as precursor. The CVD system was heated to 1000 ℃ at atmospheric pressure under 500 sccm Ar and 5 sccm H2. The precursor ammonia borane was heated to 75 ℃ by a heating belt and sublimated during the growth. After growth, the CVD system was cooled down to room temperature under the protection of mixed Ar and H2 flow.

Transfer

The GQDs synthesized in mechanically exfoliated h-BN were transferred onto SiO2/Si or commercial holey carbon film TEM grids (Zhongjingkeyi GIG-2010-3C) by regular approach using polymethyl methacrylate (PMMA). The GQDs synthesized in CVD-grown h-BN were transferred onto homemade monolayer graphene TEM Grids, which is made by transferring a large-area monolayer single-crystal graphene on commercial TEM grids mentioned above in advance.

Fabrication & Characterization methods

Milling nanopore array in h-BN was performed in Zeiss Orion NanoFab. Raman spectra were performed by HORIBA LabRAM HR800 with 633 nm laser. Photoluminescence spectra were performed by HORIBA LabRAM HR Evolution with 325 nm laser. HRTEM, STEM, SAED and EELS experiments were performed in an aberration-corrected FEI Titan Themis G2 300 operating at an accelerating voltage of 80 kV.

Conflicts of interest

The authors declare no conflict of interest.

Acknowledgements

View Article Online
DOI: 10.1039/C9NR00412B

This work was supported by National Key R&D Program of China (2016YFA0300804，2016YFA0300903), Science, Technology and Innovation Commission of Shenzhen Municipality (ZDSYS20170303165926217 and JCYJ20170412152620376), Guangdong Innovative and Entrepreneurial Research Team Program (2016ZT06D348), NSFC (51522201, 11474006 and 51672007), National Equipment Program of China (ZDYZ2015-1), Beijing Graphene Innovation Program (Z161100002116028), National Postdoctoral Program for Innovative Talents (BX201700014) and China Postdoctoral Science Foundation (2017M611148 and 2018M630017).

References

1. M. Chhowalla, H. S. Shin, G. Eda, L. J. Li, K. P. Loh and H. Zhang, *Nature Chem.*, 2013, **5**, 263-275.
2. K. S. Novoselov, A. Mishchenko, A. Carvalho and A. H. C. Neto, *Science*, 2016, **353**.
3. H. Zhang, H. M. Cheng and P. D. Ye, *Chemical Society Reviews*, 2018, **47**, 6009-6012.
4. S. De Franceschi, L. Kouwenhoven, C. Schonenberger and W. Wernsdorfer, *Nature Nanotech.*, 2010, **5**, 703-711.
5. X. Z. Lan, S. Masala and E. H. Sargent, *Nature Mater.*, 2014, **13**, 233-240.
6. Z. P. Zhang, J. Zhang, N. Chen and L. T. Qu, *Energy & Environmental Science*, 2012, **5**, 8869-8890.
7. G. Eda, Y. Y. Lin, C. Mattevi, H. Yamaguchi, H. A. Chen, I. S. Chen, C. W. Chen and M. Chhowalla, *Adv. Mater.*, 2010, **22**, 505-509.
8. X. Z. Xu, C. Liu, Z. H. Sun, T. Cao, Z. H. Zhang, E. G. Wang, Z. F. Liu and K. H. Liu, *Chemical Society Reviews*, 2018, **47**, 3059-3099.
9. C. Volk, C. Neumann, S. Kazarski, S. Fringes, S. Engels, F. Haupt, A. Muller and C. Stampfer, *Nature Commun.*, 2013, **4**.
10. X. M. Li, M. C. Rui, J. Z. Song, Z. H. Shen and H. B. Zeng, *Advanced Functional Materials*, 2015, **25**, 4929-4947.
11. V. Gupta, N. Chaudhary, R. Srivastava, G. D. Sharma, R. Bhardwaj and S. Chand, *J. Am. Chem. Soc.*, 2011, **133**, 9960-9963.
12. D. I. Son, B. W. Kwon, D. H. Park, W. S. Seo, Y. Yi, B. Angadi, C. L. Lee and W. K. Choi, *Nature Nanotech.*, 2012, **7**, 465-471.
13. D. Y. Pan, J. C. Zhang, Z. Li and M. H. Wu, *Adv. Mater.*, 2010, **22**, 734-738.
14. J. C. Ge, M. H. Lan, B. J. Zhou, W. M. Liu, L. Guo, H. Wang, Q. Y. Jia, G. L. Niu, X. Huang, H. Y. Zhou, X. M. Meng, P. F. Wang, C. S. Lee, W. J. Zhang and X. D. Han, *Nature Commun.*, 2014, **5**.
15. D. Kim, J. M. Yoo, H. Hwang, J. Lee, S. H. Lee, S. P. Yun, M. J. Park, M. Lee, S. Choi, S. H. Kwon, S. Lee, S. H. Kwon, S. Kim, Y. J. Park, M. Kinoshita, Y. H. Lee, S. Shin, S. R. Paik, S. J. Lee, S. Lee, B. H. Hong and H. S. Ko, *Nature Nanotech.*, 2018, **13**, 812-818.
16. T. Dirks, T. L. Hughes, S. Lal, B. Uchoa, Y. F. Chen, C. Chialvo, P. M. Goldbart and N. Mason, *Nature Phys.*, 2011, **7**, 386-390.
17. M. R. Connolly, K. L. Chiu, S. P. Giblin, M. Kataoka, J. D. Fletcher, C. Chua, J. P. Griffiths, G. A. C. Jones, V. I. Fal'ko, C.

G. Smith and T. J. B. M. Janssen, *Nature Nanotech.*, 2013, **8**, 417-420.
18. C. Gutierrez, L. Brown, C. J. Kim, J. Park and A. N. Pasupathy, *Nature Phys.*, 2016, **12**, 1069-1075.
19. A. El Fatimy, R. L. Myers-Ward, A. K. Boyd, K. M. Daniels, D. K. Gaskill and P. Barbara, *Nature Nanotech.*, 2016, **11**, 335-338.
20. N. M. Freitag, T. Reisch, L. A. Chizhova, P. Nemes-Incze, C. Holl, C. R. Woods, R. V. Gorbachev, Y. Cao, A. K. Geim, K. S. Novoselov, J. Burgdorfer, F. Libisch and M. Morgenstern, *Nature Nanotech.*, 2018, **13**, 392-397.
21. B. Trauzettel, D. V. Bulaev, D. Loss and G. Burkard, *Nature Phys.*, 2007, **3**, 192-196.
22. T. D. Ladd, F. Jelezko, R. Laflamme, Y. Nakamura, C. Monroe and J. L. O'Brien, *Nature*, 2010, **464**, 45-53.
23. P. Koskinen, S. Malola and H. Hakkinen, *Phys. Rev. Lett.*, 2008, **101**, 115502.
24. C. O. Girit, J. C. Meyer, R. Erni, M. D. Rossell, C. Kisielowski, L. Yang, C. H. Park, M. F. Crommie, M. L. Cohen, S. G. Louie and A. Zettl, *Science*, 2009, **323**, 1705-1708.
25. K. A. Ritter and J. W. Lyding, *Nature Mater.*, 2009, **8**, 235-242.
26. K. Kim, S. Coh, C. Kisielowski, M. F. Crommie, S. G. Louie, M. L. Cohen and A. Zettl, *Nature Commun.*, 2013, **4**, 2723.
27. J. Peng, W. Gao, B. K. Gupta, Z. Liu, R. Romero-Aburto, L. H. Ge, L. Song, L. B. Alemany, X. B. Zhan, G. H. Gao, S. A. Vithayathil, B. A. Kaipparettu, A. A. Marti, T. Hayashi, J. J. Zhu and P. M. Ajayan, *Nano Lett.*, 2012, **12**, 844-849.
28. M. Li, W. B. Wu, W. C. Ren, H. M. Cheng, N. J. Tang, W. Zhong and Y. W. Du, *Appl. Phys. Lett.*, 2012, **101**.
29. R. Q. Ye, C. S. Xiang, J. Lin, Z. W. Peng, K. W. Huang, Z. Yan, N. P. Cook, E. L. G. Samuel, C. C. Hwang, G. D. Ruan, G. Ceriotti, A. R. O. Raji, A. A. Marti and J. M. Tour, *Nature Commun.*, 2013, **4**, 2943.
30. Y. J. Xu, X. Y. Li, G. H. Hu, T. Wu, Y. Luo, L. Sun, T. Tang, J. F. Wen, H. Wang and M. Li, *Appl Surf Sci*, 2017, **422**, 847-855.
31. Y. Luo, M. Li, L. Sun, Y. Xu, M. Li, G. Hu, T. Tang, J. Wen, X. Li, J. Zhang and L. Wang, *J Colloid Interface Sci*, 2018, **529**, 205-213.
32. X. L. Zhu, W. H. Wang, W. Yan, M. B. Larsen, P. Boggild, T. G. Pedersen, S. S. Xiao, J. Zi and N. A. Mortensen, *Nano Lett.*, 2014, **14**, 2907-2913.
33. Z. Liu, L. L. Ma, G. Shi, W. Zhou, Y. J. Gong, S. D. Lei, X. B. Yang, J. N. Zhang, J. J. Yu, K. P. Hackenberg, A. Babakhani, J. C. Idrobo, R. Vajtai, J. Lou and P. M. Ajayan, *Nature Nanotech.*, 2013, **8**, 119-124.
34. L. Liu, J. Park, D. A. Siegel, K. F. McCarty, K. W. Clark, W. Deng, L. Basile, J. C. Idrobo, A. P. Li and G. Gu, *Science*, 2014, **343**, 163-167.
35. G. Kim, H. Lim, K. Y. Ma, A. R. Jang, G. H. Ryu, M. Jung, H. J. Shin, Z. Lee and H. S. Shin, *Nano Lett.*, 2015, **15**, 4769-4775.
36. L. X. Chen, L. He, H. S. Wang, H. M. Wang, S. J. Tang, C. X. Cong, H. Xie, L. Li, H. Xia, T. X. Li, T. R. Wu, D. L. Zhang, L. W. Deng, T. Yu, X. M. Xie and M. H. Jiang, *Nature Commun.*, 2017, **8**.
37. D. C. Joy, *Helium Ion Microscopy Principles and Applications*, Springer, New York Heidelberg Dordrecht London, 2013.
38. G. Hlawacek, V. Veligura, R. van Gastel and B. Poelsema, *J Vac Sci Technol B*, 2014, **32**, 020801.
39. C. Casiraghi, A. Hartschuh, H. Qian, S. Piscanec, C. Georgi, A. Fasoli, K. S. Novoselov, D. M. Basko and A. C. Ferrari, *Nano Lett.*, 2009, **9**, 1433-1441.
40. L. M. Malard, M. A. Pimenta, G. Dresselhaus and M. S. Dresselhaus, *Phys Rep*, 2009, **473**, 51-87.
41. L. A. J. Garvie, A. J. Craven and R. Brydson, *American Mineralogist*, 1994, **79**, 411-425.
42. K. Suenaga and M. Koshino, *Nature*, 2010, **468**, 1088-1090.
43. Z. Liu, L. H. G. Tizei, Y. Sato, Y. C. Lin, C. H. Yeh, P. W. Chiu, M. Terauchi, S. Iijima and K. Suenaga, *Small*, 2016, **12**, 252-259.
44. L. Liu, D. A. Siegel, W. Chen, P. Z. Liu, J. J. Guo, G. Duscher, C. Zhaog, H. Wang, W. L. Wang, X. D. Bai, K. F. McCarty, Z. Y. Zhang and G. Gu, *P Natl Acad Sci USA*, 2014, **111**, 16670-16675.
45. A. K. Geim and K. S. Novoselov, *Nature Mater.*, 2007, **6**, 183-191.
46. L. A. Ponomarenko, F. Schedin, M. I. Katsnelson, R. Yang, E. W. Hill, K. S. Novoselov and A. K. Geim, *Science*, 2008, **320**, 356-358.
47. L. B. Tang, R. B. Ji, X. K. Cao, J. Y. Lin, H. X. Jiang, X. M. Li, K. S. Teng, C. M. Luk, S. J. Zeng, J. H. Hao and S. P. Lau, *ACS Nano*, 2012, **6**, 5102-5110.
48. S. H. Jin, D. H. Kim, G. H. Jun, S. H. Hong and S. Jeon, *ACS Nano*, 2013, **7**, 1239-1245.
49. S. J. Zhu, Y. B. Song, X. H. Zhao, J. R. Shao, J. H. Zhang and B. Yang, *Nano Res*, 2015, **8**, 355-381.